COMPARATIVE CRYSTAL FIELD ANALYSIS OF THE Ni^{2+} ENERGY LEVEL SCHEME IN $CdCl_2$, $CdBr_2$, CdI_2 CRYSTALS

Mikhail G. BRIK[1], Nicolae M. AVRAM[2], Calin N. AVRAM[3]

Abstract. *The exchange charge model of crystal field was used to calculate the crystal field splitting of all Ni^{2+} energy levels ($3d^8$ electron configuration) in three structurally similar crystals of $CdCl_2$, $CdBr_2$, and CdI_2. The influence of the nature of the ligands and interionic distances on the values of the crystal field parameters and location of the split energy levels and relative intervals between them was identified. Comparison of the calculated energy levels with the experimental results available in the literature yielded good agreement.*

Keywords: Crystal field theory; Transition metal ions; Crystal field strength; Racah parameters.

1. Introduction

The transition metal ions with the unfilled 3d electron shell are widely used in various applications, such as lasing [1,2], lighting [3], optical thermometry [4,5] etc. Their absorption and emission spectra are essentially dependent on the host matrix, since the electronic states arising from the open 3d electron shell strongly interact with the nearest crystalline environment.

The theory of crystal field is a powerful tool that has been successfully applied to analyze the optical spectra of the transition metal and rare earth ions in crystals [6]. Different models of crystal field that have been developed so far allow to establish firm and deep connections between the crystal structure (the nearest surrounding of an impurity ion) and chemical nature of the surrounding ions on the one hand and the overall splitting of the impurity ion's energy levels on the other hand.

In this connection, comparative studies of the crystal field effects and impurity ions energy levels splitting for a number of similar or different systems are of special importance. For example, calculations of energy level schemes of the same impurity ion in several isostructural crystals highlight the role of the host material in the formation of the impurity ion's spectra [7, 8]. Alternatively, calculations of spectra

[1]Prof., Dr. hab., College of Sciences & CQUPT-BUL Innovation Institute, Chongqing University of Posts and Telecommunications, Chongqing, 400065, People's Republic of China; Institute of Physics, University of Tartu, W. Ostwaldi Str. 1, Tartu, 50411, Estonia; Institute of Physics, Jan Dlugosz University, PL-42200, Czestochowa, Poland, (e-mail: mikhail.brik@ut.ee).
[2]Prof., PhD, Department of Physics, West University of Timisoara, Bd. V. Parvan, No. 4, 300223, Timisoara, Romania and Academy of Romanian Scientist, Independentei 54, 050094, Bucharest, Romania (e-mail: n1m2marva@yahoo.com).
[3] Assistant Prof., PhD, Department of Physics, West University of Timisoara, Bd. V. Parvan, No. 4, 300223, Timisoara, Romania (e-mail: calin.avram@e-uvt.ro).

of several different impurity ions in the same host help to identify the whole spectral range of absorption and emission that can be realized for a given host [9, 10].

In the present paper we report on the results of applications of the exchange charge model of crystal field [11] to the calculations of the Ni^{2+} energy levels in three structurally close crystals – $CdCl_2$, $CdBr_2$, and CdI_2. Comparative discussion of the crystal field parameters and splitting of the degenerated Ni^{2+} energy levels is given. A clear trend in variation of the above-mentioned parameters and the role played by the type of ligands in these detected changes is identified and explained.

2. Crystal structure of $CdCl_2$, $CdBr_2$, CdI_2 and method of calculations

$CdCl_2$ and $CdBr_2$ crystallize in the R-3m space group (No. 166) and CdI_2 – in the $P6_3mc$ space group (No. 186). The summary of the structural properties of these crystals is given in Table 1.

Table 1) Structural parameters of the CdX_2 (X = Cl, Br, I) crystals [12].

	$CdCl_2$	*$CdBr_2$*	*CdI_2*
Space group No.	166	166	186
$a = b$, Å	3.85	3.95	4.24
c, Å	17.46	18.67	13.67
γ, º	120	120	120
Cd – X distance, Å	2.6567	2.7607	2.9854
X – Cd – X angles, º	180 (×3); 92.87 (×6); 87.13 (×6)	180 (×3); 91.35 (×6); 88.65 (×6)	180 (×3); 90.49 (×6); 89.51 (×6)

It is seen that the Cd – ligand distance increases in the Cl – Br – I direction. In each of these crystals the Cd ions are six-fold coordinated at the centers of a slightly deformed octahedron. The deformation of the coordination octahedra can be assessed in terms of the interionic distances and internal angles in the octahedron. The six Cd – X distances in each of these halides are equal, but there exists an angular distortion. In the ideal octahedron there are three X – Cd – X angles equal to 180 º and twelve X – Cd – X angles equal to 90 º. In the considered halides, however, the angles which should be 90 º deviate from this value; this deviation is the greatest in $CdCl_2$ and the smallest in CdI_2. The local symmetry at the Cd^{2+} site is D_{3d}.

Fig. 1 shows the unit cells of $CdBr_2$ (which is isostructural to that one of $CdCl_2$) and CdI_2. A common feature of all three halides is that they have a well-pronounced layered structure; the layers made of the CdX_6 octahedra are perpendicular to the c crystallographic axis. After doping, the Ni^{2+} ions occupy the Cd^{2+} sites without charge compensation.

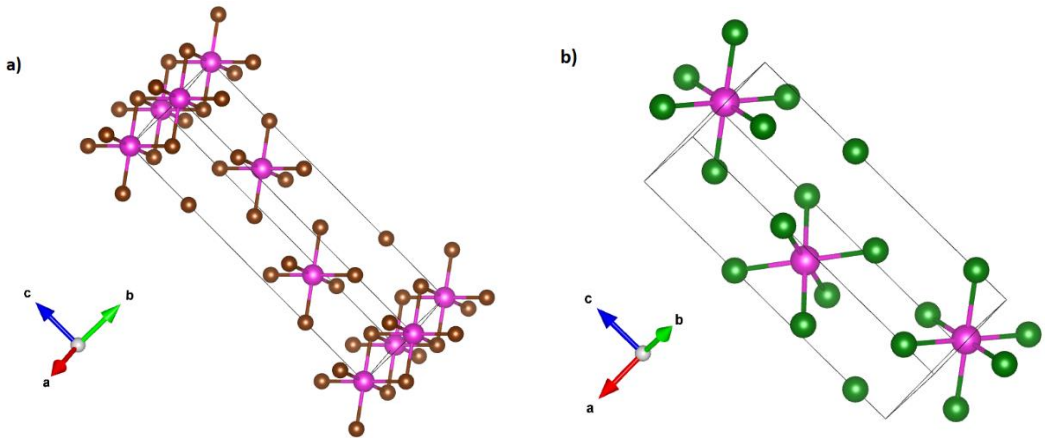

Fig. 1. a) One unit cell of $CdBr_2$ (a) and CdI_2 (b). Coordination octahedra around Zr ions are shown. Drawn with VESTA [13]. Octahedral coordination around Cd ions is shown.

The Ni^{2+} energy levels were calculated as the eigenvalues of the crystal field Hamiltonian

$$H = \sum_{p=2,4} \sum_{k=-p}^{p} B_p^k O_p^k \quad (1)$$

Here O_p^k are the linear combinations of the irreducible tensor operators acting on the angular parts of the impurity ion's wave functions (exact definition of the operators used in the exchange charge model (ECM) can be found in Refs. [11, 14), and B_p^k are the crystal field parameters (CFPs), which can be calculated from the experimentally obtained crystallographic data. The Hamiltonian (1) should be diagonalized in the space spanned by all wave functions of the free ion's LS terms arising from the Coulomb interaction between electrons of an impurity ion. In the ECM framework the CFPs are defined as a sum of two contributions [11]:

$$B_p^k = B_{p,Q}^k + B_{p,S}^k, \quad (2)$$

where

$$B_{p,Q}^k = -K_p^k e^2 \langle r^p \rangle \sum_i q_i \frac{V_p^k(\theta_i,\phi_i)}{{R_i}^{p+1}}, \quad (3)$$

$$B_{p,S}^k = K_p^k e^2 \frac{2(2p+1)}{5} \sum_i \left(G_s S(s)_i{}^2 + G_\sigma S(\sigma)_i{}^2 + \gamma_p G_\pi S(\pi)_i{}^2 \right) \frac{V_p^i(\theta_i,\phi_i)}{R_i}. \quad (4)$$

The first term $B_{p,Q}^k$ describes the electrostatic interaction between the central impurity ion and the crystal lattice ions enumerated by an index i with electrical charges q_i (in the units of the proton charge) and spherical coordinates R_i, θ_i, ϕ_i (the

reference system is centered at the impurity ion itself). The averaged values $\langle r^p \rangle$ (r is the radial coordinate of the d electrons from the unfilled electron shell of an impurity ion) can be either found in the literature or calculated numerically, using the radial parts of the corresponding ion's wave functions. The numerical factors K_p^k, γ_p, the explicit expressions for the polynomials V_p^k and the definitions of the operators O_p^k can all be found in Ref. [11].

The second term of Eq. (2) $B_{p,S}^k$ is proportional to the overlap between the wave functions of the central ion and ligands. The $S(s), S(\sigma), S(\pi)$ terms correspond to the overlap integrals between the *d*-functions of the central ion and *p*-, *s*-functions of the ligands: $S(s) = \langle d0|s0\rangle, S(\sigma) = \langle d0|p0\rangle, S(\pi) = \langle d1|p1\rangle$. The G_s, G_σ, G_π entries are the ECM dimensionless adjustable parameters. Their numerical values are determined from the positions of the first three absorption bands in the experimental spectrum. A good approximation is to assume them to be equal, $G_s = G_\sigma = G_\pi = G$; then only the lowest in energy absorption band is sufficient to find the value of *G* [11]. The summation in Eq. (4) includes the nearest neighbors of an impurity ion only (i.e. six/four ligands in the case of an octahedral/tetrahedral impurity center), because the overlap of the wave functions decreases rapidly with the distance and is important for the nearest neighbors only.

Despite a small number of fitting parameters employed in the ECM, it is possible to calculate the crystal field parameters and energy levels of impurities in crystals without invoking any assumptions about the impurity center symmetry, and with high accuracy. Many examples of successful applications of the ECM to the calculations of energy level of the rare earth ions [11, [14] and references therein] and transition metal ions [**Eroare! Marcaj în document nedefinit.**,15,16, 17 and references therein] can be found in the literature.

3. Ni^{2+} ions: energy levels in a free state and in a crystal fields of O_h and D_{3d} symmetries

Ni^{2+} ions have the following electron configuration: $1s^2 2s^2 2p^6 3s^2 3p^6 3d^8$. The completely filled electron shell are not optically active, and the main optical properties are determined by the $3d^8$ electron configuration (if the high-lying 4s, 4p states are not considered).

The Coulomb repulsion between the 3d electrons gives rise to 5 LS terms: two spin-triplets ^{3}F (the ground state) and ^{3}P and three spin-singlets ^{1}D, ^{1}G, ^{1}S. Their relative energies are expressed in terms of the Racah parameters for a free ion B_0, C_0 as follows (if the energy of the ^{3}F term is taken as zero): $15B_0$ for ^{3}P, $5B_0 + 2C_0$ for ^{1}D, $12B_0 + 2C_0$ for ^{1}G, and $22B_0 + 7C_0$ for ^{1}S (the subscript "0" indicates that these

values are for free ions; when the ions with unfilled electron shells are embedded into the solids, the values of the Racah parameter are reduced due to the nephelauxetic effect [18]).

In a crystal field these energy levels are split into a number of sublevels, whose degree of degeneracy and symmetry properties of their wave functions can be analyzed with the help of the group theory [1, 17]. Table 2 below shows the splitting of these LS terms for the O_h group and D_{3d} group (the latter one is the point symmetry of the Ni^{2+} ions in the considered hosts).

Table 2) Splitting of the orbitally degenerated states (the values of the orbital momenta *L* are given in the parenthesis) of the $3d^8$ electron configuration in the crystal fields with the O_h and D_{3d} local symmetries. The entries in the parenthesis in the D_{3d} column show the splitting of the corresponding entries in the O_h column.

	O_h	D_{3d}
S (*L*=0)	A_{1g}	A_1
P (*L*=1)	T_{1g}	$A_2 + E$
D (*L*=1)	$T_{2g} + E_g$	$(A_1 + E)$ + (E)
F (*L*=3)	$A_{2g} + T_{1g} + T_{2g}$	(A_2) + $(A_2$ + E) + $(A_1 + E)$
G (*L*=4)	$A_{1g} + E_g + T_{1g} + T_{2g}$	(A_1) + (E) + $(A_2$ + E) + $(A_1 + E)$

The quantitative analysis of the energy levels of d ions in crystal fields with the cubic (O_h or T_d) symmetry is based on the Tanabe-Sugano diagrams [19]. Since three parameters are needed in this case to calculate all energy levels positions (the crystal field strength *Dq*, Racah parameters *B* and *C*), these diagrams express the energy of the crystal field states in the units of the Racah parameter *B* versus the *Dq*/*B* ratio for the fixed *C*/*B* ratio.

Fig. 2 shows the Tanabe-Sugano diagram for the d^8 electron configuration in the octahedral crystal field for the *C*/*B* ratio equal to 4.5. When *Dq*/*B* = 0, the free ion energy level scheme is obtained. When *Dq*/*B* > 0, all energy levels become split in accordance with the data from Table 2. The energy interval between the ground state $^3A_{2g}$ and the first excited spin-triplet state $^3T_{2g}$ (both come from the ground term ^{3}F) is equal in this case to 10*Dq* value [19], which gives an easy way of experimental determination of the crystal field strength for the d^2 and d^8 electron configurations.

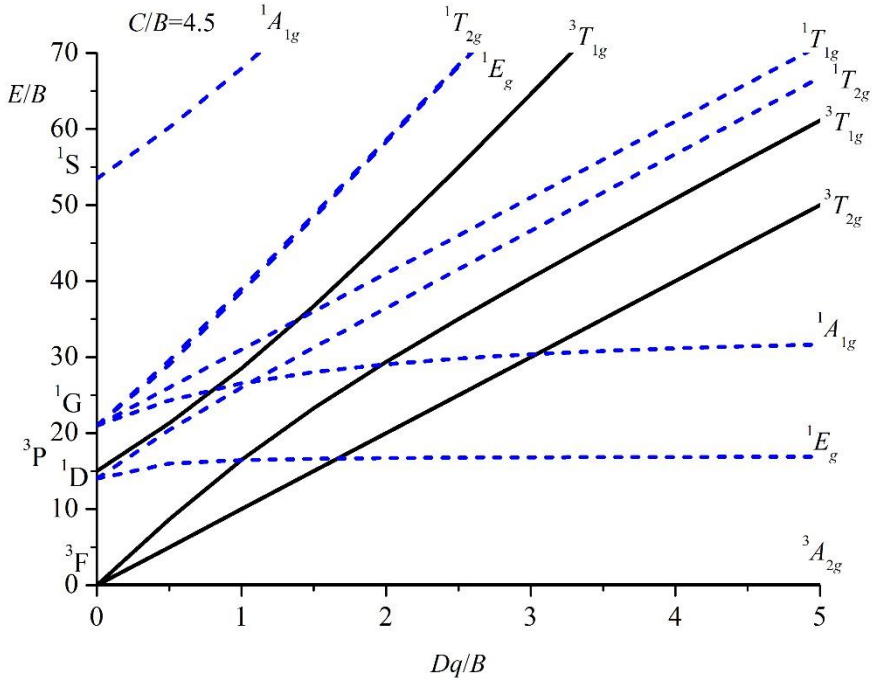

Fig. 2. The Tanabe-Sugano diagram for the d^8 electron configuration in the octahedral crystal field. The solid and the dashed lines show the spin-triplet and spin-singlet states, respectively.

4. Results of calculations

The structural data from Ref. [12] were used to create large clusters consisting of 25221 ions in $CdCl_2$ and $CdBr_2$ and 24338 ions in CdI_2, to ensure convergence of the crystal lattice sums needed to calculate the point charge contributions to the CFP. The overlap integrals between the wave functions of the Ni^{2+} and Cl^-, Br^-, I^- ions were calculated numerically using the radial parts of their wave functions from Ref. [20] and were approximated by the exponential functions, whose equations are given in Table 3 [7].

The non-zero calculated CFP are collected in Table 4. The trigonal symmetry of the crystallographic site occupied by the Ni^{2+} ions is reflected by the structure of the crystal field Hamiltonian, in which only three CFP - B_2^0, B_4^0, B_4^3 differ from zero. The eigenvalues of the crystal field Hamiltonian (1) with the CFP from Table 4 are collected in Table 5, in comparison with the available experimental and theoretical data.

Table 3) The Ni^{2+} - X^- (X = Cl, Br, I) overlap integrals (R is the Ni^{2+} - X^- distance in atomic units). .

	Ni^{2+} - Cl^-	Ni^{2+} - Br^-	Ni^{2+} - I^-
$S(s) = \langle d0 \vert s0 \rangle$	-1.82070 exp(-0.85599R)	1.53760 exp(-0.79983R)	1.22140 exp(-0.72022R)
$S(\sigma) = \langle d0 \vert p0 \rangle$	0.81606 exp(-0.59570 R)	0.57804 exp(-0.51055R)	0.49431 exp(-0.46882R)
$S(\pi) = \langle d1 \vert p1 \rangle$	1.54200 exp(-0.85907 R)	1.42630 exp(-0.81434R)	1.33490 exp(-0.76824 R)

Table 4) Calculated CFP (in cm^{-1}, Stevens's normalization) for Ni^{2+} ions in $CdCl_2$, $CdBr_2$ and CdI_2 crystals. Q, S, and Total stand for the $B^k_{p,Q}$, $B^k_{p,S}$ and total CFP, correspondingly. The values of the non-dimensional ECM parameter G and Racah parameters B, C (in cm^{-1}) are also given.

	$CdCl_2$			*$CdBr_2$*			*CdI_2*		
	Q	*S*	*Total*	*Q*	*S*	*Total*	*Q*	*S*	*Total*
B^0_2	1261	-540	721	1341	-239	1102	1152	-83	1069
B^0_4	-72	-1096	-1168	-63	-1071	-1134	-45	-1070	-1115
B^3_4	-1669	-34555	-36224	-1360	-31790	-33150	-911	-30776	-31687
G			15.12			15.45			21.0
B			800			600			825
C			3470			3670			3250

It is seen from Table 4 that the Racah parameters are considerably reduced to the free Ni^{2+} ion values (B_0 = 1068 cm^{-1}, C_0 = 4457 cm^{-1} [21]), which indicates high degree of covalence in all considered materials.

The overall agreement between the calculated and experimentally detected energy levels shown in Table 5 is good. It should be emphasized that only one fitting parameter G of the ECM is sufficient to reach such a good correlation with the experimental data; no assumptions for the local symmetry of the impurity center was made, but only the crystal structure data were used as an input for the crystal field calculations. The obtained CFP values also allowed to analyze the crystal field splitting in terms of the D_{3d} point group irreducible representations by using the symmetry descent approach from the parent O_h to the actual D_{3d} symmetry.

Table 5) Calculated energy levels (in cm^{-1}, Stevens's normalization) for Ni^{2+} ions in $CdCl_2$, $CdBr_2$ and CdI_2 crystals. The orbital doublet states are denoted with an asterisk.

		$CdCl_2$			*$CdBr_2$*			*CdI_2*		
		Exp.[a]	*Calc.*[b]	*Calc.*[c]	*Exp.*[a]	*Calc.*[b]	*Calc.*[c]	*Exp.*[d]	*Calc.*[b]	*Calc.*[d]
$^3A_{2g}$ (^{3}F)	$^3A_2$	0	0	0	0	0	0	0	0	0
$^3T_{2g}$ (^{3}F)	$^3A_1$ ^3E	7200	6983*, 7457	7140 7231	6645	6456*, 7014	6645 6659	6350-7100	6240*, 6728	6320-7140
$^3T_{1g}$ (^{3}F)	^3E $^3A_2$	11365	11849*, 12116	11869 12029	10616, 11416	10770, 10887*	10982 11005	11200	10718, 10884*	10520-11300
^1E_g (^{1}D)	^1E	12920	12845*	12264	11820	11826*	11218	12540	12514*	12510
$^1T_{2g}$ (^{1}D)	$^1A_1$ ^1E		19441*, 19923	19005 19179	16800	17981*, 18271	17550 18547		18292*, 18899	
$^1A_{1g}$ (^{1}G)	$^1A_1$	19200	20602	19748	18116	18760	18072		20149	
$^3T_{1g}$ (^{3}P)	$^3A_2$ ^3E	21700, 22200	21185*, 22256	20653 21090	20580	17608*, 19273	19228 19293		20276*, 21842	
$^1T_{1g}$ (^{1}G)	$^1A_2$ ^1E		23560*, 23997	22843 22931		21038*, 21554	21003 21017		22621*, 23128	
^1E_g (^{1}G)	^1E		28702*	28232		25826*	25990		27016*	
$^1T_{2g}$ (^{1}G)	^1E $^1A_1$		28713, 29885*	28604 28798		26017, 27419*	26316 26275		27019, 28486*	
$^1A_{1g}$ (^{1}S)	$^1A_1$		52147	50313		48419	46108		50015	

[a] Ref. [22]; [b] This work; [c] Ref. [23] [d] Ref. [24]

The calculated values of *Dq* (which were estimated from the barycenters of the states coming from the $^3T_{2g}$ state) are 714 cm^{-1} for $CdCl_2$:Ni^{2+}, 664 cm^{-1} for $CdBr_2$:Ni^{2+}, and 640 cm^{-1} for CdI_2:Ni^{2+}. These values are in good agreement with the experimental estimations of 720 cm^{-1} for $CdCl_2$:Ni^{2+} [22], 640 cm^{-1} for $CdBr_2$:Ni^{2+} [22] and 666 cm^{-1} for CdI_2:Ni^{2+} [24].

The decrease of the calculated *Dq* parameter in the $CdCl_2$ – $CdBr_2$ – CdI_2 sequence follows the increase of the interionic distances in the same direction.

The *Dq*/*B* ratios are equal to 0.89 for $CdCl_2$:Ni^{2+}, 1.10 for $CdBr_2$:Ni^{2+}, and 0.78 for CdI_2:Ni^{2+}, which indicates that a weak crystal field case is realized in each of the considered systems.

5. Conclusions

Three cadmium halide crystals – $CdCl_2$, $CdBr_2$ and CdI_2, doped with the Ni^{2+} ions – were considered in this paper. The crystal field parameters for the Ni^{2+} ions were calculated using the exchange charge model of crystal field, and the obtained values were used to diagonalize the crystal field Hamiltonian to get the Ni^{2+} energy levels. The D_{3d} local symmetry of the crystallographic site occupied by the impurity ions in all three studied compounds is reflected in the structure of the crystal field Hamiltonian and the pattern of the energy levels splitting. The agreement between the calculated and experimentally detected energy levels for these systems was good. A decrease of the crystal field strength with increased anion atomic number was explained by increased interionic distances.

Acknowledgment

M.G.B. thanks the supports from the Chongqing Recruitment Program for 100 Overseas Innovative Talents (Grant No. 2015013), the Program for the Foreign Experts (Grant No. W2017011) and Wenfeng High-end Talents Project (Grant No. W2016-01) offered by Chongqing University of Posts and Telecommunications (CQUPT), Estonian Research Council grant PUT PRG111, European Regional Development Fund (TK141) and NCN project 2018/31/B/ST4/00924.

References

[1] R.C. Powell, *Physics of Solid-State Laser Materials* (Springer, Berlin, 1998).
[2] S. Kück, Appl. Phys. B **72**, 515 (2001).
[3] Q. Zhou, L. Dolgov, A. M. Srivastava, *et al*., J. Mater. Chem. C **6**, 2652 (2018).
[4] J. Ueda, M. Back, M. G. Brik, *et al.,* Opt. Mater. **85**, 510 (2018).
[5] C. Matuszewska, L. Marciniak, J. Lumin. **223**, 117221 (2020).
[6] D.J. Newman, B. Ng (Eds.), *Crystal Field Handbook* (Cambridge, 2000).
[7] M. G. Brik, N. M. Avram, C. N. Avram, Physica B **371**, 43 (2006).
[8] M. G. Brik, K. Ogasawara, Phys. Rev. B **74**, 045105 (2006).
[9] M. G. Brik, N. M. Avram, J. Phys. Chem. Solids **67**, 1599 (2006).
[10] M. G. Brik, N. M. Avram, J. Phys.: Condens. Matter **21**, 155502 (2009).
[11] B.Z. Malkin, in: A.A. Kaplyanskii, B.M. Macfarlane (Eds.), Spectroscopy of Solids Containing Rare-earth Ions, North-Holland, Amsterdam, 1987, pp. 13–50.
[12] R. W. G. Wyckoff, Cryst. Struct. **1**, 239 (1963).
[13] K. Momma, F. Izumi, J. Appl. Crystallogr. **44** 1272 (2011).
[14] B. Z. Malkin, N. M. Abishev, E. I. Baibekov, D. S. Pytalev, K. N. Boldyrev, M. N. Popova, M. Bettinelli, Phys. Rev. B 96 (2017) 014116.
[15] M.G. Brik, A.M. Srivastava, Opt. Mater. 54 (2016) 245.
[16] A.M. Srivastava, M.G. Brik, Opt. Mater. 63 (2017) 207.

[17] M. G. Brik, C.-G. Ma, *Theoretical Spectroscopy of Transition Metal and Rare Earth Ions: From Free State to Crystal Field* (Jenny Stanford Publishing, Singapore, 2020).
[18] C. J. Jørgensen, *Absorption spectra and chemical bonding in complexes* (Pergamon Press, Oxford, 1962).
[19] S. Sugano, Y. Tanabe, H. Kamimura, *Multiplets of Transition-Metal Ions in Crystals*, (Acad. Press, New York and London, 1970).
[20] E. Clementi, C. Roetti, At. Data Nucl. Data Tables **14**, 177 (1974).
[21] P. H. M. Uylings, A. J. J. Raasen, J. F. Wyart, J. Phys. B **17**, 4103 (1984).
[22] J. Ackerman, C. Fouassier, E. M. Holt, S. L. Holt, Inorg. Chem. **11**, 3118 (1972).
[23] Y.-R. Zhao, X.-Y. Kuang, C. Lu, *et al*., Mol. Phys. **107**, 133 (2009).
[24] S. R. Kuindersma, P. R. Boudewijn, C. Haas, Phys. Stat. Sol. B **108**, 187 (1981).